Mice homozygous for a targeted disruption of the proto-oncogene *int-2* have developmental defects in the tail and inner ear

Suzanne L. Mansour, Judy M. Goddard and Mario R. Capecchi

Howard Hughes Medical Institute, Department of Human Genetics, University of Utah School of Medicine, Salt Lake City, UT 84112, USA

SUMMARY

We derived mice that carry a targeted insertion of a *neo^r* gene in the *int-2* (*Fgf-3*) proto-oncogene coding sequences. The mutation was found to be recessive and mice that were homozygous for the insertion did not often survive to adulthood. The mutant mice had defects in the development of the tail and inner ear that could be correlated with disruption of *int-2* expression in the posterior primitive streak and hindbrain or otic vesicle. While the tail phenotype was 100% penetrant, we found that the inner ear phenotype had reduced penetrance and variable expressivity. The variable expressivity could not be attributed to variability in the genetic background of the mutant allele or to leaky expression from the mutant allele. Thus, we conclude that even in a uniform genetic background, stochastic variation in the expression of a developmental circuit can result in dramatic differences in phenotypic consequences.

Key words: *int-2*, *Fgf-3*, proto-oncogene, gene targeting, gene disruption, ES cells, tail, inner ear, developmental mutant

INTRODUCTION

The *int-2* gene (also designated *Fgf-3*) is a member of the fibroblast growth factor (FGF) gene family, which currently comprises seven members. Membership in this family is defined by a highly conserved 120 amino acid core. The FGFs are secreted proteins that bind to cell-surface and extracellular-matrix heparan sulfate proteoglycans. This binding may serve to restrict the distribution of the FGFs to the vicinity of the cells that produce them and appears to modulate their interactions with the high-affinity FGF receptor family. The FGFs have a wide range of mitogenic and differentiation promoting activities in a variety of assay systems; however, their precise role in any particular biological process with which they have been associated remains speculative (reviewed by Burgess and Maciag, 1989; Goldfarb, 1990; Baird and Klagsbrun, 1991; Ruoslahti and Yamaguchi, 1991).

Unlike the other members of the FGF family, the *int-2* gene was originally identified because its transcription was activated by the nearby integration of mouse mammary tumor virus (MMTV) proviral DNA in a large number of virus-induced mammary tumors (Dickson et al., 1984). This finding, in addition to the amino acid sequence homology to the FGFs (Dickson and Peters, 1987), suggested that *int-2* might be involved in controlling the growth of mammary cells. Indeed, introduction of an MMTV-driven *int-2* transgene into the mouse genome does induce mammary hyperplasia (Muller et al., 1990). However, *int-2* expression has not been detected in any non-neoplastic adult tissue, suggesting that these ectopic expression studies do not address its normal role in the animal.

Northern blot and in situ hybridization analyses (Jakobovits et al., 1986; Wilkinson et al., 1988, 1989; Niswander and Martin, 1992) have detected *int-2* mRNAs at a wide variety of sites in the developing mouse embryo, suggesting a number of possible roles for *int-2* during development. Between embryonic days 6.25 to 9.5 (E6.25-E9.5), *int-2* mRNA was detected in an extraembryonic tissue, the parietal endoderm, and in both extraembryonic and embryonic (primitive streak) migrating mesoderm (Wilkinson et al., 1988; Niswander and Martin, 1992). In addition, *int-2* RNA was detected in the hindbrain rhombomeres 5 and 6, adjacent to the otocyst (the primordium of the inner ear), as well as in the pharyngeal pouches (Wilkinson et al., 1988). In studies of older embryos (E10.5 to E17.5) and newborn pups (P0), *int-2* expression was detected in the developing cerebellum, retina, teeth and inner ear (Wilkinson et al., 1989). *int-2* mRNAs potentially encode two proteins; one initiated at a CUG codon located upstream from and in-frame with a traditional AUG-initiated open reading frame (Acland et al., 1990). However, it is not known which, if either, of these proteins, is actually produced by any of the tissues that normally express *int-2* mRNA.

The hindbrain rhombomeres in which *int-2* mRNAs are detected have been implicated as the source of an inductive signal required for the formation and subsequent devel-

opment of the otocyst (reviewed by Van De Water and Ruben, 1976; Van De Water et al., 1980; Noden and Van De Water, 1986; Van De Water and Represa, 1991). Because it has the properties expected of a signaling molecule and is presumably produced by the inducing tissue, Int-2 protein has been proposed as a candidate for the otocyst-inducing signal (Wilkinson et al., 1988). This idea has been tested by culturing chick hindbrain and otic placode explants in vitro in the presence of anti-sense oligonucleotides complementary to the presumed site of translation initiation on *int-2* mRNA. In those experiments, the antisense oligonucleotides prevented otocyst formation (Represa et al., 1991).

We have taken a direct, genetic approach to understanding the role of *int-2* in development that does not depend on any prior assumptions about its function. The *int-2* gene was disrupted in mouse embryonic stem (ES) cells by targeting a *neo*[r] gene into the first protein-coding exon (Mansour et al., 1988). Mice heterozygous for the mutated gene were derived from one of the targeted cell lines and were intercrossed to generate homozygous mutant offspring. We report here that the targeted allele is recessive and that homozygous *int-2* mutant mice do not often survive to adulthood. These mice have defects in both tail and inner ear development that become apparent around embryonic day 11.5. The tail defect arises from abnormalities of the mesoderm derived from the posterior primitive streak. The mutant mice have no defect in the induction of the otocyst per se; rather, their inner ear abnormalities are largely a consequence of the failure of the otocyst to form an endolymphatic duct.

MATERIALS AND METHODS

Generation of *int-2*[neo] and *int-2*[lacZ] mice

The isolation of ES cell lines that carry a targeted insertion of a *neo*[r] poly(A)⁻ expression cassette or a *lacZ/neo*[r] poly(A)⁺ cassette into *int-2* exon 1b at an *Apa*I site converted to *Xho*I was exactly as described previously (Mansour et al., 1988, 1990). The targeted cell lines used to generate the reported mice were analyzed extensively by Southern blot hybridization using a variety of restriction enzymes, and both flanking and internal probes. The results were identical to those published previously for cell lines 43-8H (*neo*[r] cassette) and 62-8K (*lacZ/neo*[r] cassette), and demonstrated that all of the targeted cell lines had been altered by the predicted replacement of endogenous sequences by vector sequences. One of the resulting cell lines carrying the *neo*[r] poly(A)⁻ insertion, 46-6H, was used to generate *int-2*[neo] mice, also as described previously (Thomas and Capecchi, 1990). Another cell line, 87-1H, carrying the *lacZ/neo*[r] insertion, was used to generate *int-2*[lacZ] mice. See Fig. 1 and below for Southern blot hybridization analysis of tail DNA from heterozygotes, compound heterozygotes and homozygous mutants. The population of heterozygotes was expanded by breeding the initial carriers of the mutant alleles to C57Bl/6 mice. Intercross litters were obtained by pairing male and female heterozygotes overnight. The day that a copulation plug was observed was considered E0.5 and the day of birth was designated P0.

Genotype assays

DNA was prepared by phenol and chloroform extraction of proteinase K-digested yolk sacs or tails from *int-2*[neo] intercross
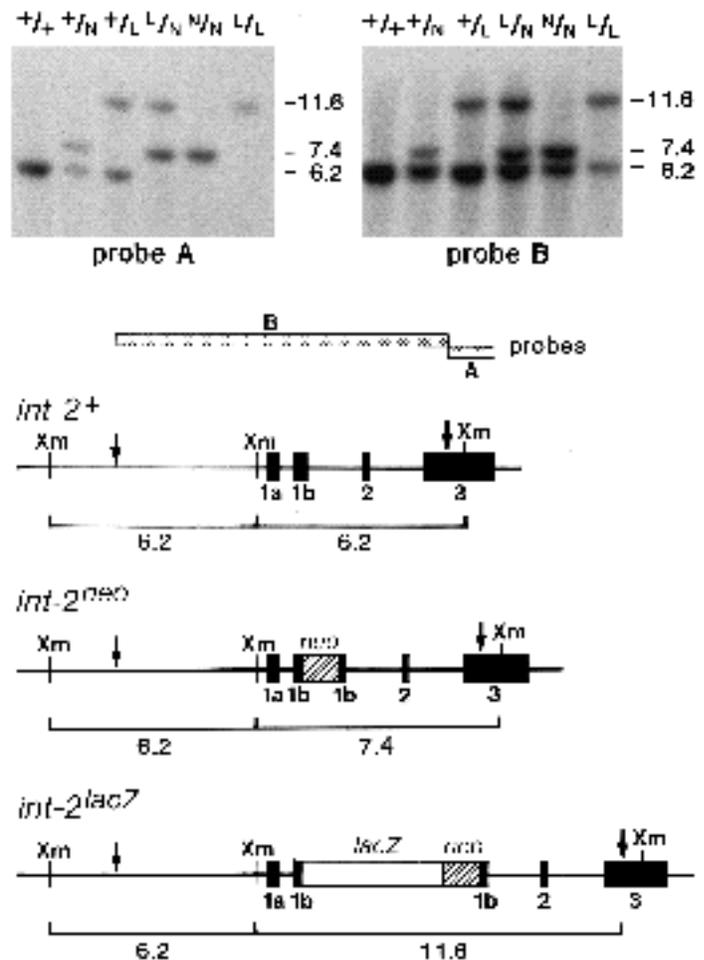

Fig. 1. Southern blot hybridization distinguishes between all offspring of +/*int-2*[neo] and +/*int-2*[lacZ] parents. Tail DNAs from homozygous wild-type (+/+), heterozygous *int-2*[neo] (+/N), heterozygous *int-2*[lacZ] (+/L), compound heterozygous (L/N), homozygous *int-2*[neo] (N/N) and homozygous *int-2*[lacZ] (L/L) mice were digested with *Xmn*I, gel fractionated, blotted and hybridized with probe A, the 1.3 kb 3′ cDNA probe, and probe B, the 10 kb genomic probe. Maps of the wild-type (*int-2*⁺), *int-2*[neo] and *int-2*[lacZ] alleles are shown below the filters. The probes are indicated with dotted boxes. The sites of *Xmn*I (Xm) digestion are shown. Arrows delimit the ends of the *int-2* sequences carried by the targeting vectors used to create the mutant alleles. Filled boxes indicate *int-2* exons, hatched boxes represent the *neo*[r] gene and the open box represents the *lacZ* gene.

embryos or pups (Hogan et al., 1986). DNA samples were digested with *Hin*dIII and *Xho*I, subjected to electrophoresis in 0.75% agarose gels, blotted onto nylon (GeneScreen, DuPont/NEN) and u.v.-crosslinked with 1800 μjoules (Stratalinker, Stratagene). The filter was hybridized as described (Church and Gilbert, 1984) with the addition of 15% formamide. The probe was a random-primed, ³²P-labeled (Pharmacia kit) 1.3 kb *Eco*RI DNA fragment from the 3′ untranslated sequences of the *int-2* cDNA, c.72 (Mansour and Martin, 1988). When *int-2*[neo] heterozygotes were crossed with *int-2*[lacZ] heterozygotes, the genotypes of the offspring were determined by hybridizing *Xho*I and *Hin*dIII digested yolk sac DNAs with a 10 kb genomic *int-2* probe that contains all of the *int-2* sequences carried by the targeting vectors (data not shown, but see Mansour et al., 1988, 1990), or by hybridizing *Xmn*I-digested

yolk sac DNAs with the 3′ flanking cDNA probe (Fig. 1, probe A). Either of these procedures allows us to distinguish uniquely all of the possible genotypes resulting from any of the three possible intercross configurations. In addition, hybridization of *Xmn*I-digested tail DNA with the 10 kb genomic probe (Fig. 1, probe B) showed that the only restriction fragments detected were those uniquely predicted from a homologous replacement of endogenous *int-2* sequences with targeting vector sequences.

Histology
Embryos

Following cervical dislocation of pregnant females, the conceptuses were removed and dissected free of decidua in phosphate-buffered saline (PBS). The yolk sacs were saved in DNA isolation buffer (Hogan et al., 1986) for later genotype analysis and the embryos were stored in Bouin's fixative at 4°C.

Adult ears

Adult animals were perfused through the heart with 4% formaldehyde, 0.1 M Na/Na$_2$ PO$_4$ pH 7.2. The inner ears were dissected and then decalcified in 0.1 M EDTA pH 7.2, 2% formaldehyde. All tissues were dehydrated through a graded ethanol series, cleared in xylene, and then infiltrated and embedded in Paraplast X-tra (Polysciences). Sections were stained regressively with hematoxylin and eosin and mounted in DPX (Aldrich).

Skeleton staining

Newborn animals were killed by asphyxiation in CO$_2$. The carcasses were eviscerated, fixed in 95% ethanol, and stained with alizarin red S to reveal bone and alcian blue to reveal cartilage (McLeod, 1980). They were subsequently cleared by trypsin digestion and KOH treatment, and stored in glycerol (Dingerkus and Uhler, 1977).

Whole-mount β-galactosidase detection and anti-neurofilament staining

E9.5 embryos from crosses between *int-2^{neo}* and *int-2^{lacZ}* heterozygotes were dissected in PBS and then fixed in 0.1 M Pipes pH 6.9, 2 mM MgCl$_2$, 1.25 mM EGTA, 2% formaldehyde (C. Cepko, personal communication) for 6 minutes at room temperature. Embryos were rinsed three times in PBS and one time in tissue-staining buffer (Sanes et al., 1986) without X-gal (5-bromo-4-chloro-3-indolyl-β-D-galactopyranoside). Embryos were then incubated in tissue-staining buffer containing 1 mg/ml X-gal, overnight at 37°C. No regions of endogenous β-galactosidase activity were detected in these embryos. After staining, the embryos were rinsed in PBS and refixed in 4% formaldehyde in PBS for 10 minutes. Immunostaining with the 2H3 anti-155×10^3 M_r neurofilament monoclonal antibody (Dodd et al., 1988) was performed as described (Chisaka et al., 1992). Photography of whole embryos was done with transillumination on a dissecting microscope. Doubly stained embryos were processed for paraffin embedding as described above. Sections were dewaxed, rehydrated and counterstained for 30 seconds in 0.02% nuclear fast red, 5% Al$_2$(SO$_4$)$_3$·(14-18)H$_2$O, then dehydrated through an ethanol series and mounted in DPX.

Reverse transcriptase-polymerase chain reaction assay of *int-2* transcripts

E9.5 embryos from *int-2^{lacZ}* intercrosses were dissected free of decidua, quick frozen in liquid N$_2$ and stored at −80°C. The genotype of each embryo was determined using yolk sac DNA as described above. Total RNA was isolated from individual embryos

using the guanidinium thiocyanate/LiCl method (Cathala et al., 1983). A similar preparation of RNA from four E9.5 SW embryos showed that each embryo contained approximately 5 μg of total RNA. The RNA from each embryo was reverse transcribed with the MuLV enzyme (BRL) using random hexamers to prime the synthesis and 300 ng of the resulting cDNA was amplified in the presence of [α-^{32}P]dCTP in an Air Thermo-Cycler (Idaho Technologies) according to Tan and Weis (1992). PCR products were resolved on a 6% acrylamide/8M urea DNA sequencing gel. Band intesities were quantified after exposure of the gel in a phosphorimager (Molecular Dynamics) and the signals generated from the *int-2* primer pairs were normalized to the actin signal from each cDNA sample. The primers used were: β-actin-5′ 5′-GGGTCA-GAAGGACTCCTATG-3′; β-actin-3′ 5′-GTAACAATGCCAT-GTTCAAT-3′; int-2-A 5′-GATGGGCCTGATCTGGC-3′; int-2-B 5′-CGCAGTAATCTCCAGGATGC-3′; int-2-C 5′-TGGTG-GCGTTTACGAGCACC-3′. The actin pair was amplified for 14 cycles, using 0 seconds denaturation at 94°C, 0 seconds annealing at 59°C and 4 seconds extension at 72°C. Pilot experiments showed that *int-2* amplification was exponential between 20 and 25 cycles, so we used 22 cycles in the experiment shown. The C/B primer pair was amplified using the same conditions as for the actin pair. The A/B primer pair was amplified using 0 seconds denaturation at 94°C, 0 seconds annealing at 62°C and 6 seconds extension at 72°C.

RESULTS

Insertion of a *neo^r* cassette into the mouse *int-2* gene causes a recessive mutation

The *int-2* gene was disrupted in CC1.2 ES cells by the targeted insertion of a selectable *neo^r* expression cassette into the first protein-coding exon, as described previously (Mansour et al., 1988). The *neo^r* gene employed was driven by the MC1 promoter (Thomas and Capecchi, 1987), but lacked a polyadenylation signal, which was provided by the downstream *int-2* sequences. The *neo^r* gene was positioned within exon 1b, several codons downstream from the signal peptide-coding sequence (see Fig. 1 for a map of the targeted allele). This site was chosen to prevent the production of secreted forms of Int-2 protein by separating the sequences coding for both Int-2 translation initiation sites and the signal peptide from those that encode the rest of the protein. Thus the targeted allele, designated *int-2^{neo}*, was expected to be a null.

An ES cell line heterozygous for the *int-2^{neo}* allele was injected into C57Bl/6 blastocysts which were then implanted into pseudo-pregnant females. The resulting chimeric males were tested for their ability to transmit the ES cell-derived agouti coat color to their offspring. One of the chimeras sired agouti offspring that carried the *int-2^{neo}* allele and these were used to establish a family of heterozygous carriers. None of these animals, regardless of the sex of the parent from which they received their mutant allele, had any obvious abnormalities.

To assess the consequences of homozygosity for the *int-2* mutation, we intercrossed heterozygotes. The resulting embryos were collected between 9.5 and 18.5 days of gestation and genotyped using Southern blot hybridization to distinguish between the wild-type and mutant alleles (see Materials and methods). Of a total of 194 embryos from 28 intercross litters we found 43 homozygous wild-type
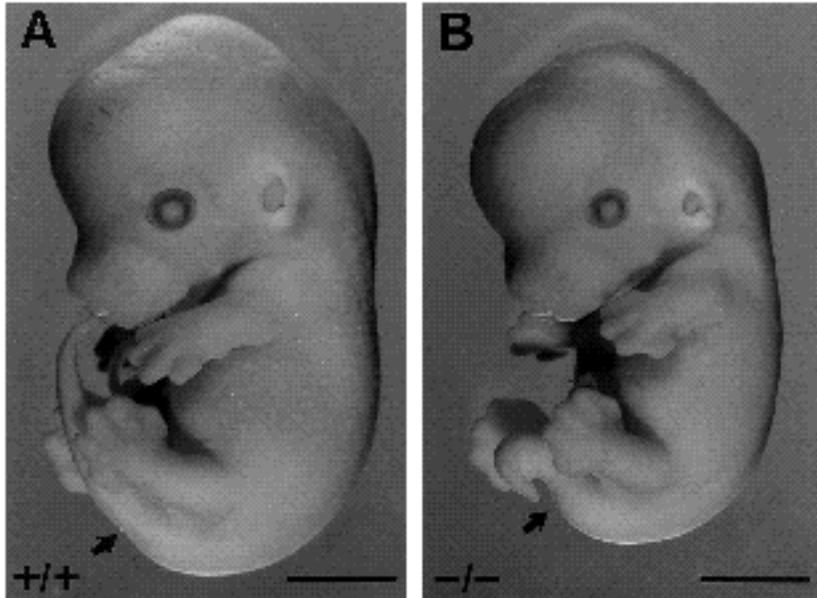
Fig. 2. *int-2* mutant embryos have abnormal tails. Two E13.5 *int-2^neo* intercross littermates are shown. (A) Homozygous wild-type (+/+) embryo. (B) Homozygous mutant (−/−) embryo. In each case, the tail is indicated with an arrow. Bar, 2 mm.

(+/+), 102 heterozygous (+/*int-2^neo*) and 49 homozygous mutant (*int-2^neo*/*int-2^neo*) embryos. These results fit the Mendelian expectation for the segregation of an allelic pair. Homozygous mutant embryos were found on each day of gestation that was examined, including the day prior to birth (E18.5).

The *int-2^neo* mutants have tail defects

Beginning at E12.5, all homozygous mutant embryos had a visible defect consisting of an abnormally short, curly or kinked tail. Fig. 2 shows an E13.5 homozygous wild-type embryo with a normal tail (Fig. 2A) and a homozygous mutant littermate with a short, dorsally curled tail (Fig. 2B). Such tails were never seen on wild-type or heterozygous embryos. At E9.5 and E10.5, we were not able to distinguish the homozygous mutants from their littermates by visual inspection. At E11.5, however, about 50% of the homozygous mutants could be identified by the tail phenotype. At this stage, the identifiably mutant tails always curled dorsally. In older mutant embryos, the direction of curling was not consistent. In contrast to a number of other mouse mutants with abnormal tails (Copp et al., 1990), the *int-2* mutant embryos never showed evidence of an open neural tube. In addition to having an abnormal tail, the homozygous mutants from E12.5 and onward were smaller than their normal littermates (compare Fig. 2B and 2A). These embryos also appeared to be developmentally younger than their normal littermates. For example, the mutant embryo in Fig. 2B had not yet developed hair follicles and had somewhat shallower interdigital clefts than its control littermate in Fig. 2A. The extent of the size diminution and developmental delay was quite variable and has not been quantified. However, when considering control embryos for histological analysis (presented below), we always chose ones that were as developmentally similar to the mutants as possible.

int-2^neo mutants often die in the early postnatal period

We next examined the consequences of the *int-2^neo*/*int-2^neo* genotype on postnatal life. Litters born from heterozygote intercrosses were checked within 24 hours of birth and an attempt was made to ensure the survival of all offspring and to obtain tissue samples for genotype analysis if they did not survive. A total of 197 pups were observed from 26 intercrosses. Twenty-three (12%) of these had very short, curly or kinked tails and were smaller than their normal littermates (data not shown). We were able to genotype 163 of the intercross offspring and found 45 (28%) homozygous wild-type, 100 (61%) heterozygous and 18 (11%) homozygous mutant pups. As for the E12.5 and older intercross embryos, we found that the homozygous mutant genotype was concordant with a tail defect. However, the number of homozygous mutants was only one half of that expected. Since there appeared to be little or no embryonic lethality, we assume that the missing homozygous mutants must have been consumed by their mothers at some time very shortly after birth.

The 18 genotyped *int-2* mutant pups and the 5 pups presumed to be mutant based on their tail phenotype, survived for varying lengths of time. Eleven (48%) of them lived for less than two days, including five that were found dead within 24 hours of birth. Another seven mutants (30%) lived for between two days and three weeks. It has not been possible to determine a specific cause of death for these mutants. However, although animals sighted alive on the day of birth were clearly capable of breathing and nursing, they often appeared immature relative to their littermates and this may have compromised their survival. Five mutants (22%), all females, survived to weaning. In contrast, about 76% of the animals with a normal phenotype survived to weaning or were deliberately killed as controls. Two of the surviving female mutants were tested for fertility in a cross with a heterozygous male. Both animals proved to be fer-
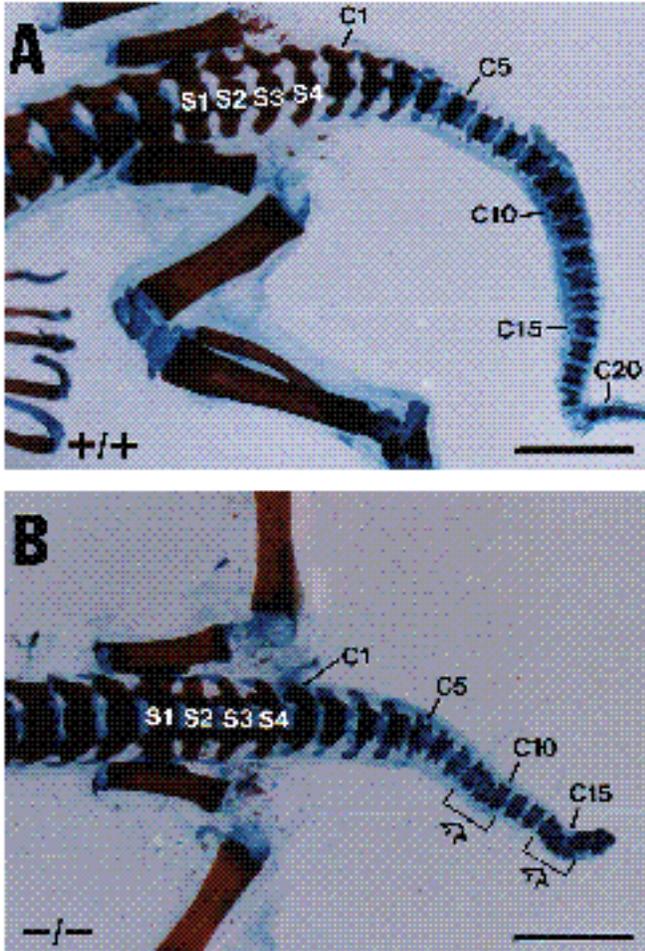
Fig. 3. Caudal regions of P1 mutant skeletons have abnormal vertebrae. (A) Homozygous wild-type (+/+) pup. (B) Homozygous mutant (−/−) pup. Skeletons were stained with alcian blue and alizarin red S and cleared as described (Dingerkus and Uhler, 1977; McLeod, 1980). Cartilage is blue and bone is red. The pelvic bones were removed so that the sacral vertebrae (S1-S4) could be seen clearly. These vertebrae appear normal in both skeletons. The caudal vertebrae are indicated with a C. The arrows and brackets show regions with fused or abnormally shaped caudal vertebrae. The apparent kink in the tail of the wild-type pup was caused when the skin was being removed. Bar, 2 mm.

tile and between them produced a total of 9 normal heterozygous pups and 7 homozygous mutant pups with the tail defect.

The *int-2^neo* mutants have abnormal caudal vertebrae

To examine the nature of the tail defects, we prepared cleared skeletons from seven P0 to P4 mutants as well as from littermate controls and stained them to visualize cartilage (blue) and bone (red). Fig. 3 shows the skeletons of a P1 heterozygote and a homozygous mutant. As expected, the mutant's trunk vertebrae, of which the four sacral ones are indicated, were normal (Fig. 3B). The first four to seven caudal (tail) vertebrae were also normal in the mutant skele-

ton. The rest of the mutant's tail showed abnormally shaped and/or fused vertebrae that had not begun to ossify. In kinked tails, such as the one shown, stretches of normally shaped vertebrae were interspersed with abnormally shaped vertebrae. The number of caudal vertebral units varied from 9 to 23 in the mutants (29 is normal), and the pattern of fusions and malformations was different for each of the seven mutants that were examined (data not shown).

Formation of the tail begins at about E9.5, when primary neurulation is nearing completion. The tail grows out from the tail bud which contains the remnants of the primitive streak. An undifferentiated mesenchyme, produced by cell division, begins to organize dorsally and cavitate, forming the neural tube of the tail in a process called secondary neurulation. The tail notochord and gut grow out as extensions of those structures in the trunk. These form somewhat later than the tail neural tube, so that they do not extend as far caudally in the tail as does the neural tube (Schoenwolf, 1977, 1984). The subsequent condensation and differentiation of the remaining mesenchyme to form the tail somites is similar to the same process in the trunk. As in the trunk, the most caudal regions of the tail are developmentally the youngest.

The *int-2* mutant tail phenotype first became visibly evident in some of the E11.5 animals and, at this stage, all of the precursors of the caudal vertebrae should have been formed. Therefore, to explore the embryological origins of this phenotype, we prepared transverse sections of dissected tails from E11.5 control (Fig. 4A-D) and mutant (Fig. 4E-H) embryos. We chose mutant tails with only a very slight dorsal curl, so that transverse sections would not cut through the tail twice. The organization of the mutant tails was quite abnormal. In contrast with normal tails (Fig. 4A), the gut tube extended more caudally in the mutant tail than did the neural tube and notochord (Fig. 4E). In addition, caudal sections from mutant tails (Fig. 4F,G) had a larger separation between the notochord and gut tube, as well as a greater area, than was seen in normal sections (Fig. 4B,C) located the same distance from the tail tip. Also, an approximately 250 μm segment of the mutant tail had very disorganized somites with no clear demarcation between left and right sides (compare Fig. 4B,F). In some sections of the mutant tail, it appeared that somite blocks had formed on top of each other (Fig. 4G). From examination of the entire set of sections, it was clear that this feature was not due to an oblique sectioning plane. At more cranial levels, the mutant tail structure became more normal (Fig. 4H), until eventually it was indistinguishable from the control (Fig. 4D). In addition, the mutant tails had an abnormally large neural tube, especially in the most caudal regions of the tail (compare Fig. 4F,G with Fig. 4B,C).

The *int-2^neo* mutants have inner ear defects

One of the homozygous *int-2^neo* mutant survivors had several abnormal behaviors. She was hyperactive compared with her littermates and moved in circles. Her head was tilted consistently to the right although she circled in both directions. She had difficulty righting herself when placed on her back, but showed a marked improvement in this skill by five weeks of age relative to her performance at three weeks of age (data not shown). In addition, she showed
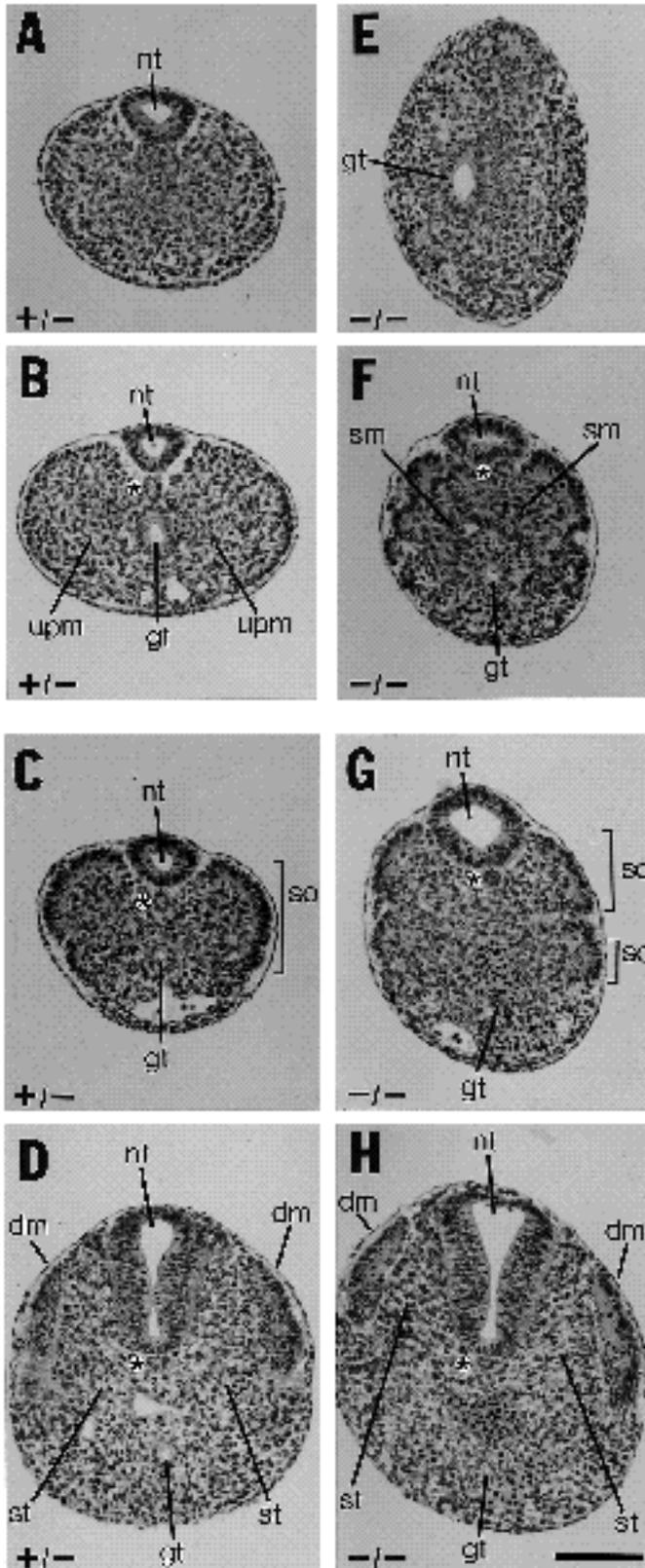
Fig. 4. The *int-2^neo* tail phenotype is apparent at E11.5. (A-D) 5 μm transverse sections from an E11.5 heterozygous (+/−) tail. (E-F) 5 μm transverse sections from the tail of a mutant (−/−) littermate. Sections were stained with hematoxylin and eosin and arranged vertically in caudal to cranial order. Adjacent panels, A and E, B and F, and C and G, show sections from the same position relative to the tip of the tail. D is much more cranial than H, but they were similarly located with respect to the base of the tail. nt (neural tube); gt (gut tube); upm (unsegmented paraxial mesoderm); sm (segmented mesoderm); so (somite), dm (dermomyotome); st (sclerotome). The notochord is to the right of the asterisk. Bar, 100 μm.

matic behavioral phenotype. Nevertheless, they have all been retarded in their ability to right themselves, even though they all eventually learned this skill. One of them showed some tendency to circle and one seemed unresponsive to the crude hearing tests that we applied. These behaviors were never noted for any of the wild-type or heterozygous offspring of a +/*int-2^neo* intercross. From 12 subsequent unmonitored intercrosses, a total of eight more homozygous mutants, four males and four females, survived to weaning. Three of these animals also exhibited the abnormal behaviors described above.

Since the behavioral phenotype described above is characteristic of mouse mutants with inner ear defects (Deol, 1968, 1980; Steel et al., 1983), we killed the animal described above, along with a littermate control, and processed the inner ears for histological analysis (Fig. 5). Comparison of mid-modiolar sections viewed at low magnification showed gross deformations in both of the mutant inner ears (Fig. 5B,C). Neither the osseous nor the membranous labyrinth had a normal structure. Nevertheless, analysis of serial sections permitted identification of most of the expected structures in the mutant's right ear (Fig. 5B). However, the cochlea appeared to be improperly coiled, and both the cochlear duct and the semicircular canals were enlarged. Examination of sections at higher magnification showed that both cochlear and vestibular portions of the inner ear had developed sensory epithelia, although the spiral ganglia that would normally innervate the cochlear hair cells were severely reduced in number (data not shown). The mutant's left ear (Fig. 5C) was more extremely affected. It appeared to be composed of two cochlear chambers, each lined by the stria vascularis, but only one of which showed development of the organ of Corti (the sensory epithelium responsible for hearing). No spiral ganglion cells could be found in that ear.

int-2 is not required for induction of the otocyst

In normal mice, the inner ear begins as a thickening of the ectoderm (auditory placode) in the region of the presumptive hindbrain. This region invaginates to form the otic cup and subsequently becomes covered with surface ectoderm, so that it forms a closed otic vesicle (otocyst) adjacent to rhombomeres 5 and 6 of the hindbrain (Rugh, 1968; Theiler, 1989; Kaufman, 1990). This process is thought to require an inductive signal from the hindbrain (reviewed by Van De Water and Ruben, 1976; Van De Water et al., 1980; Noden and Van De Water, 1986; Van De Water and Represa, 1991). We examined a total of six mutant embryos

little or no ear movement in response to clicking noises from behind and had little tendency to startle in response to an unseen hand clap (Preyer's reflex). The other four homozygous mutant survivors have not shown such a dra-
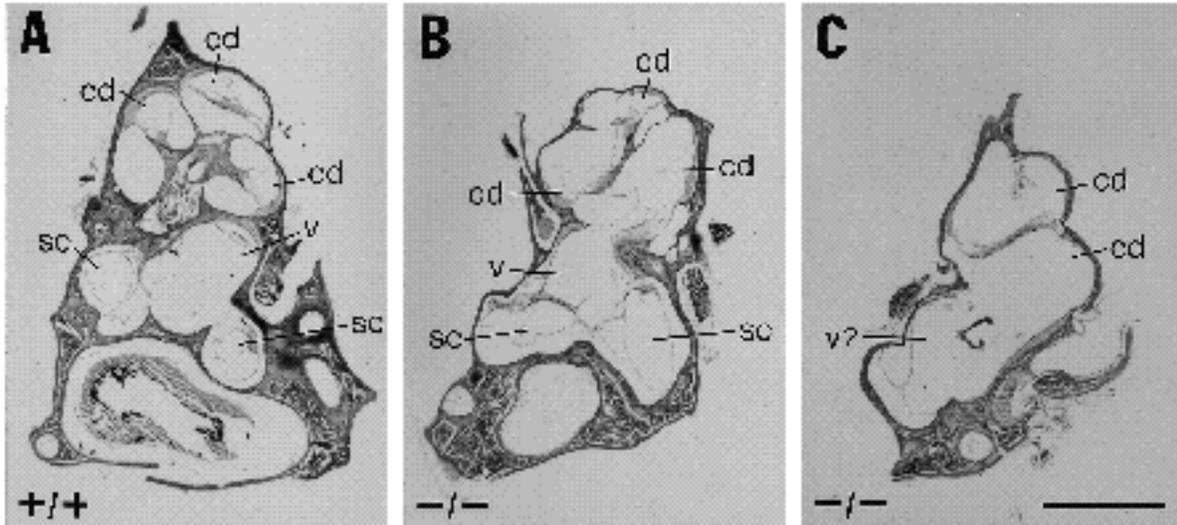
Fig. 5. Adult *int-2^neo* mutants have inner ear defects. Hematoxylin and eosin-stained 10 μm mid-modiolar sections of (A) homozygous wild-type (+/+) right inner ear, (B) homozygous mutant (−/−) right inner ear and (C) −/− left inner ear. cd (cochlear duct); v (vestibule); sc (semi-circular canal). Bar, 1 mm.

at the otic vesicle stage (E9.5) and could not find any abnormality in the structure or position of the otic vesicle relative to wild-type or heterozygous controls. Fig. 6 shows transverse sections through the otocyst of a homozygous wild-type embryo (Fig. 6A) and a homozygous mutant embryo (Fig. 6B). Examination of these and other serial sections showed that these two embryos were virtually identical.

In addition to the size and location of the otocyst itself, we also examined the size and location of the VII-VIIIth ganglion complex as well as the structure of hindbrain rhombomeres 5 and 6, which express *int-2* mRNA and which have been suggested to be the source of the otocyst-inducing signal. To identify the *int-2*-expressing cell types, even in *int-2* mutants, we made use of mice that express an *E. coli lacZ* reporter gene under the control of the endogenous *int-2* control elements. *int-2^lacZ* mice were generated from ES cells that carried a targeted insertion of a *lacZ/neo^r* cassette into *int-2* exon 1b as previously described (Mansour et al., 1990, see also Materials and methods). Like *int-2^neo* heterozygotes, the *int-2^lacZ* heterozygotes have a normal phenotype, but they express *E. coli* β-galactosidase in a pattern that reflects the expression of *int-2* mRNA (manuscript in preparation). As expected, animals homozygous for this independently derived *int-2^lacZ* allele, as well as the compound heterozygotes (*int-2^neo/int-2^lacZ*), have phenotypes indistinguishable from homozygous *int-2^neo* mice, because the *lacZ/neo^r* cassette also disrupts *int-2* in the first protein-coding exon.

We crossed *int-2^neo* heterozygotes with *int-2^lacZ* heterozygotes, collected embryos at E9.5 and then stained them with X-gal to reveal the sites of β-galactosidase expression. All of the E9.5 embryos (21-25 somites) that carried the *int-2^lacZ* allele, regardless of whether the other allele was wild type (Fig. 6C) or *int-2^neo* (Fig. 6D), showed the same staining pattern. Consistent with the restricted expression of *int-2* mRNA (Wilkinson et al., 1988), a short

segment of the neural tube, immediately adjacent to the otocyst, was the only region of the embryo that expressed detectable levels of β-galactosidase at this stage.

In order to visualize the developing cranial nerves and ganglia, the X-gal-stained embryos were subsequently immunostained with an antibody directed against neurofilaments (Dodd et al., 1988). Fig. 6E and F show photographs of the same embryos shown in Fig. 6C and D, respectively. Again, we were unable to see any consistent differences between embryos that had a +/*int-2^lacZ* genotype (Fig. 6E) and those which had an *int-2^neo/int-2^lacZ* genotype (Fig. 6F). A coronal section taken through the ventral region of the otocyst of an *int-2^neo/int-2^lacZ* embryo is shown in Fig. 6G. The mutant otocyst appeared to be appropriately located adjacent to rhombomeres 5 and 6, which had blue crystals of X-gal product indicative of *int-2* expression, along the luminal and pial surfaces. In addition, the morphology of the mutant rhombomeres appeared normal, as did the primordial VII-VIIIth ganglion, which appears brown from the immunostain. Further examination of serial sections from this and other matched pairs of control and mutant embryos revealed no significant effects of the *int-2* mutant genotype on the otocyst, hindbrain or VII-VIIIth ganglion at E9.5.

int-2 is involved in the induction of the endolymphatic duct

At E10.5 to E11.5 the endolymphatic duct pinches off from the dorsomedial aspect of the otic vesicle (Rugh, 1968; Sher, 1971; Theiler, 1989; Kaufman, 1990). This component of the inner ear is thought to be involved in regulating fluid (endolymph) pressure in the membranous labyrinth (Guild, 1927; Hendriks and Toerien, 1973). Also at this stage, the VII-VIIIth ganglion complex enlarges, especially in the ventral direction, and, by E11.5, the single ganglion mass begins to split into distinct VII (facial) and VIII (acoustic) components (Sher, 1971).

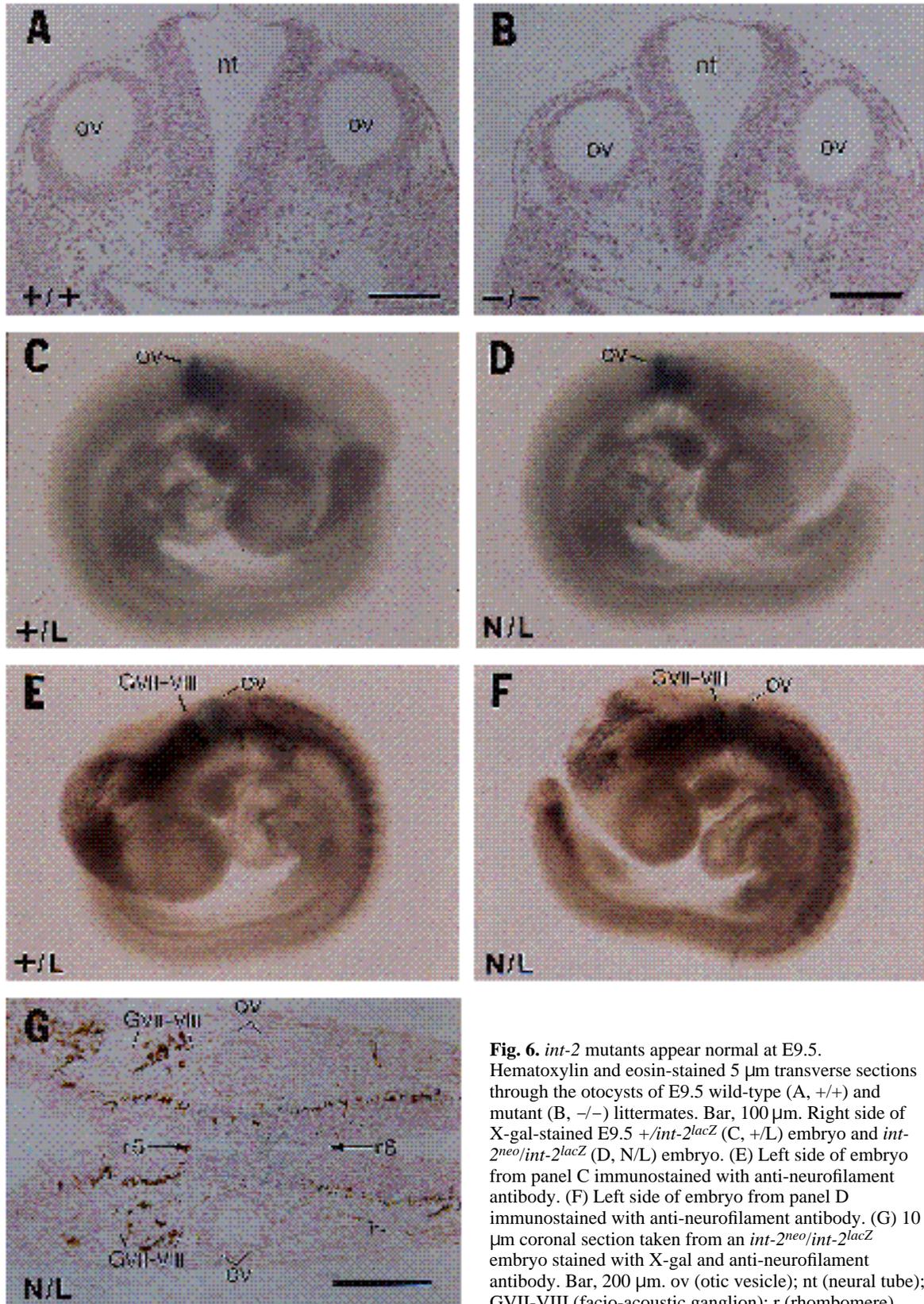Fig. 7 shows transverse sections taken through the oto-

Fig. 6. *int-2* mutants appear normal at E9.5. Hematoxylin and eosin-stained 5 µm transverse sections through the otocysts of E9.5 wild-type (A, +/+) and mutant (B, −/−) littermates. Bar, 100 µm. Right side of X-gal-stained E9.5 +/*int-2^lacZ* (C, +/L) embryo and *int-2^neo*/*int-2^lacZ* (D, N/L) embryo. (E) Left side of embryo from panel C immunostained with anti-neurofilament antibody. (F) Left side of embryo from panel D immunostained with anti-neurofilament antibody. (G) 10 µm coronal section taken from an *int-2^neo*/*int-2^lacZ* embryo stained with X-gal and anti-neurofilament antibody. Bar, 200 µm. ov (otic vesicle); nt (neural tube); GVII-VIII (facio-acoustic ganglion); r (rhombomere).

cysts of E10.5 and E11.5 heterozygous and homozygous mutant *int-2^neo* embryos. At E10.5, even the control embryos had not yet begun to form an endolymphatic duct, and the heterozygous (Fig. 7A) and homozygous mutant (Fig. 7B) littermates shown here both had appropriately located otocysts. This was also the case for the three other
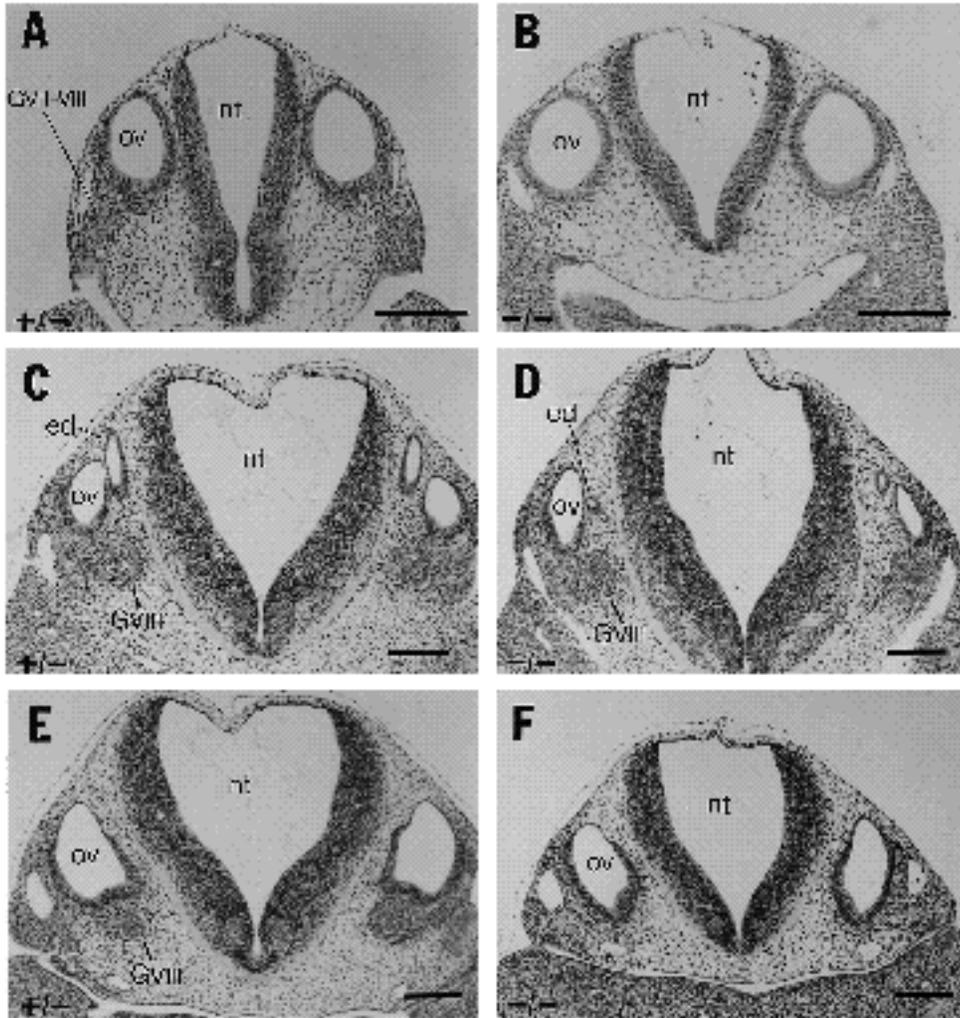
Fig. 7. *int-2^{neo}* mutant embryos have defects in the acoustic ganglion and fail to induce an endolymphatic duct. Transverse sections (7 µm) of heterozygous (+/−) and homozygous mutant (−/−) E10.5 (A and B, Bar, 200 µm) and E11.5 (C-F, Bar, 200 µm) embryos taken through the otocyst and stained with hematoxylin and eosin. C and D are located slightly more anteriorly than E and F. nt (neural tube); ov (otic vesicle); ed (endolymphatic duct); GVII-VIII (facio-acoustic ganglion); GVIII (acoustic ganglion).

homozygous mutants examined at E10.5 The embryos could be distinguished, however, by examining the VII-VIIIth ganglion. The mutant ganglion (Fig. 7B) was much smaller than the control ganglion (Fig. 7A), so that it did not even appear in this section, which was chosen so that the relative positions of the otocysts could be compared. Examination of serial sections showed that the ganglion was not entirely missing, but that its remaining component was simply located anterior to the section shown. Two of four E10.5 mutants that we examined showed a diminution of the facio-acoustic ganglion; the others appeared normal.

By E11.5, a normal endolymphatic duct was clearly present in all of the control embryos that we examined (Fig. 7C). In three out of four *int-2^{neo}* homozygous mutant embryos, the endolymphatic duct was severely reduced in size (Fig. 7D), but it was always possible to find at least a slight outpocketing on the otocyst, showing where the duct would normally form. In addition, the two otocysts in the mutant shown did not appear to be identical to each other with respect to the extent of endolymphatic duct formation, although it is difficult to quantify that impression without carrying out a detailed reconstruction.

One of the E11.5 mutant embryos also showed an appar-

ently symmetric defect in the size of the VIIIth ganglion. Fig. 7E shows a transverse section of a heterozygous embryo taken posterior to that in Fig. 7C. The comparable section from a mutant embryo does not reveal any VIIIth ganglion cells in this region (Fig. 7F). As with the E10.5 mutants, it was necessary to examine more anterior sections in order to find the diminished mutant ganglion.

int-2^{neo} mutants develop hydrops of the inner ear

The subsequent stages in the development of the inner ear become increasingly complex. The ventral portion of the otocyst continues to elongate and coil, eventually through $1\frac{3}{4}$ turns, to form the cochlea. The specialized sensory epithelium of the cochlea, known as the organ of Corti, begins to differentiate at about E12.5 and does not attain its final form until P10. The vestibular system, which develops from the dorsal portion of the otocyst, also attains its mature shape in the period between E12.5 and E16.5. The semicircular canals, the planes of which are approximately perpendicular to each other, are all present by E13.5. Their specialized sensory epithelia (the cristae) form on E13.5, but continue to differentiate until P1. The chamber that separates the cochlea from the semicircular ducts divides into two parts, the saccule and the utricle by
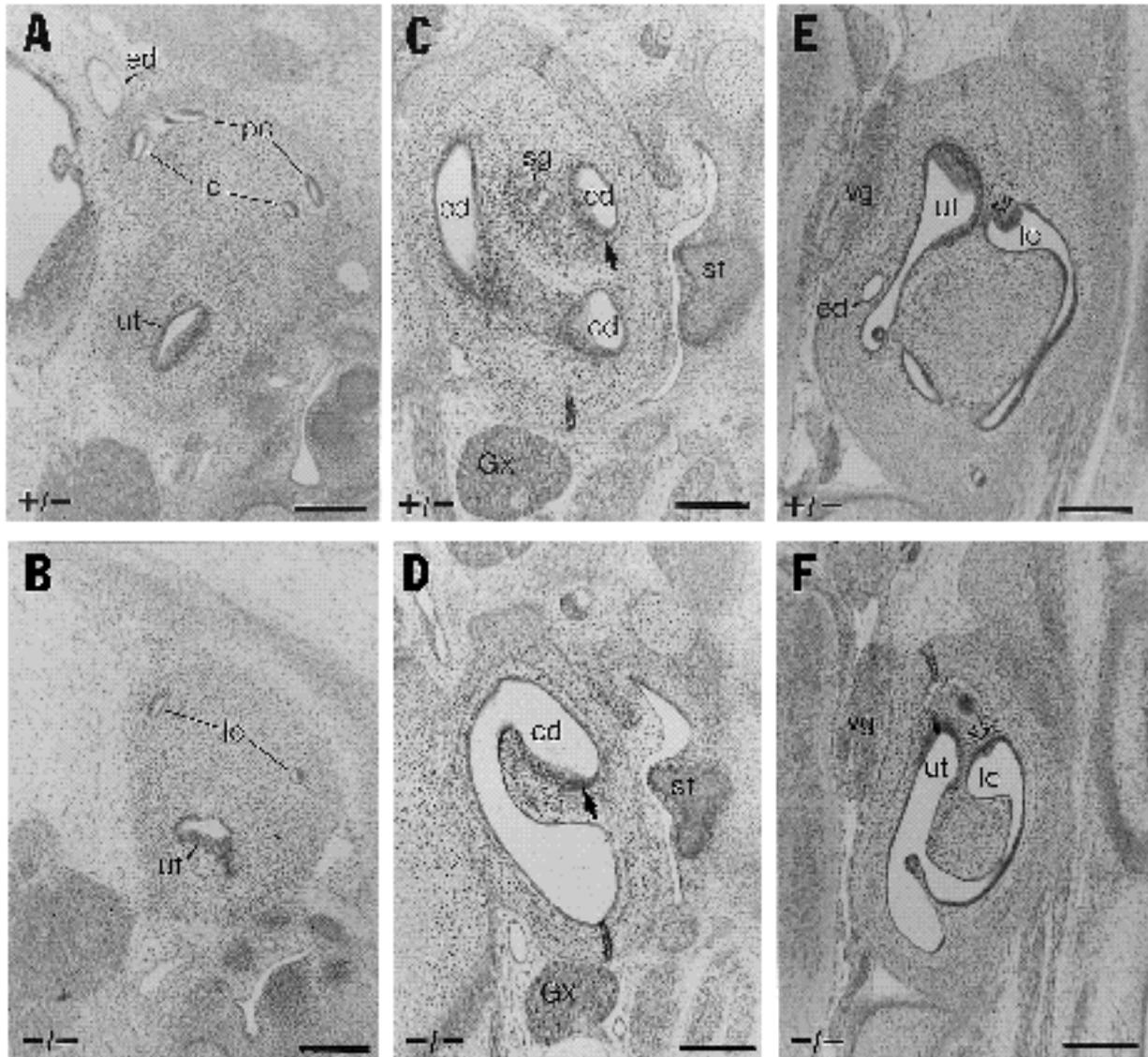
Fig. 8. Inner ear defects in E13.5 and E15.5 *int-2^neo* mutant embryos. Sagittal sections (7 µm) taken through the vestibular portion of the inner ear of E13.5 heterozygous (A, +/−) and homozygous mutant (B, −/−) embryos. Bar, 300 µm. Transverse sections (7µm) taken through the cochlear (C and D) and vestibular (E and F) portions of E15.5 heterozygous (+/−) and homozygous mutant (−/−) embryos. The developing organ of Corti (C and D) is indicated with an arrow. The crista in each lateral canal (E and F) is indicated with an arrow. Bar, 200 µm. ed (endolymphatic duct); ut (utricle); lc (lateral canal); pc (posterior canal); sg (spiral ganglion); cd (cochlear duct); st (stapes); GX (tenth ganglion); vg (vestibular ganglion).

E14.5. These two chambers have a third type of sensory epithelium, the macula, which can be recognized at E13.5 but which also continues to differentiate until the day of birth (Sher, 1971).

The inner ear defects in the *int-2* mutants examined between E12.5 and P0 were very heterogeneous with respect to the affected portion of the inner ear. Sagittal sections taken through the inner ears of two E13.5 littermates (Fig. 8) show that expected structures were sometimes missing. While sections from the heterozygote appeared normal (Fig. 8A), it is clear that the mutant (Fig. 8B) lacked an endolymphatic duct and sac, and was also missing, or had a greatly reduced, posterior semicircular canal.

The most characteristic property of *int-2^neo* mutant inner

ears was a distention (hydrops) of the affected structure. Fig. 8C shows a transverse section taken through the cochlea of an E15.5 heterozygote. A similar section taken from a homozygous mutant littermate (Fig. 8D) shows that the cochlear duct was not a neatly coiled tube but instead, a distended sac. The epithelium in a small region did show the normal thickening to 5 or 6 cell layers characteristic of a developing organ of Corti. However, spiral ganglion cells could not be found in this ear.

A similar distention of the vestibular portions of the E15.5 mutant ear was apparent. The utricle and saccule showed no sign of a division into two parts (data not shown) and the semicircular canals were dilated in the mutant (Fig. 8F). We found that the sensory regions of the epithelium

characteristic of the appropriate vestibular region had begun to differentiate. For example, a crista was apparent in the lateral semicircular canal in both the heterozygous and mutant embryo sections (Fig. 8E,F). In contrast to the spiral ganglion, it was apparent that the vestibular division of the VIIIth ganglion was similar in both embryos. Finally, examination of numerous mutant embryonic inner ears has not revealed any significant deformation in the structure of the otic capsule. The development of the auditory regions of the brain did not appear to be affected either.

The *int-2^neo* inner ear phenotype is often asymmetric

The observed heterogeneity of the *int-2^neo* inner ear phenotype between individuals (penetrance) can also be seen between the two sides of a single embryo (expressivity). Fig. 9 shows examples of mutant embryos with symmetric defects (Fig. 9A,B), asymmetric defects, (Fig. 9C-F) and mutant embryos with no apparent inner ear defects (Fig. 9G,H). Two coronal sections taken through the cochlear region of the inner ear of a heterozygous (Fig. 9A) and a mutant embryo (Fig. 9B) illustrate the symmetric class of mutants. Note that none of the structures other than the inner ear appeared to be affected. Sagittal sections taken through the cochlear region of a heterozygous (Fig. 9C,E) and a mutant (Fig. 9D,F) embryo illustrate the asymmetric class of mutants. In this case, one mutant cochlea (Fig. 9D) was apparently unaffected, whereas the other cochlea (Fig. 9F) showed the distention and lack of coiling observed in many mutants. Finally, we occasionally encountered embryos that were mutant as judged by their genotype and tail phenotype (Fig. 9H) but which nevertheless had inner ears judged to be normal relative to littermate controls (Fig. 9G). Of a total of 14 E11.5 to P0 serially sectioned mutant embryos, we found five with symmetric defects, six with asymmetric defects and three that had two normal appearing inner ears.

Normal *int-2* transcripts are not produced by homozygous mutant embryos

The variability in the *int-2* inner ear phenotype prompted us to ask whether the mutant allele could express transcripts encoding Int-2 protein. To address this issue, we prepared total RNA from individual *int-2^lacZ* intercross embryos at E9.5 and then assayed for *int-2* transcripts that linked the *int-2* AUG initiation codon in exon 1b (primer A, upstream of the inserted sequences, Fig. 10D) to exon 2 (primer B, downstream of the inserted sequences, Fig. 10D) by using a quantitative reverse transcriptase-polymerase chain reaction (PCR) assay (Tan and Weis, 1992). The expected 241 bp PCR product was observed when cDNA from a homozygous wild-type embryo was amplified (Fig. 10A). This product was reduced by about 1.5-fold when cDNA from a heterozygous embryo was assayed. The 241 bp PCR product was not detectable when cDNA from two different homozygous mutants was assayed. As expected, cDNA from an adult spleen was also negative in the assay. The fact that equivalent amounts of cDNA were used in each PCR assay was verified by the similarity of the band intensities generated with a pair of primers specific for actin cDNA (Fig. 10C). When the same cDNAs were assayed

using one primer in exon 1b (primer C, Fig. 10D), downstream of the *neo^r* insertion and one primer in exon 2 (primer B, Fig. 10D), the expected 145 bp PCR product was obtained with wild-type and heterozygous cDNA, in an approximately two to one ratio. This product was also detected, at 20- to 30-fold reduced levels, in cDNA prepared from the homozygous mutants, but was undetectable in adult spleen cDNA (Fig. 10B). Since the 145 bp product could not have been produced from cDNAs that included upstream exon 1b sequences, they must be derived from cDNAs initiated within the inserted sequences, presumably at the *neo^r* promoter. Expression of Int-2-related polypeptides from such a message would require reinitiation of translation on a bicistronic message. Translation initiation at the first in-frame methionine codon in *int-2* exon 2 would result in the synthesis of a peptide lacking 40% of the normal Int-2 sequences, including 40% of the FGF-homologous core, as well as a signal peptide. Furthermore, 5 to the in-frame methoinine codon in exon 2, there are out-of-frame initiation and temination codons that would interfere with such a hypothetical reinitiation mechanism. Thus we conclude that the *int-2^lacZ* allele is not likely to be leaky. Because this allele produced the same mutant phenotypes as the *int-2^neo* allele, the latter is not likely to be leaky either.

DISCUSSION

The *int-2* gene has been proposed to be involved in a variety of developmental processes based on its complex expression pattern in the mouse embryo (Jakobovits et al., 1986; Wilkinson et al., 1988; Wilkinson et al., 1989), and its homology with the other members of the FGF gene family (Dickson and Peters, 1987). As a step toward understanding the role of *int-2* in development, we generated mice that carried an insertion of a *neo^r* expression cassette or a *lacZ* reporter gene in the first *int-2* protein coding exon. This insertion in exon 1b was expected to generate a null mutation because it dissociates the *int-2* initiation codon and signal peptide coding sequences from the rest of the *int-2* open reading frame, precluding the production of full-length Int-2 protein. Since mice heterozygous for the *int-2^neo* and the *int-2^lacZ* alleles were phenotypically normal, we conclude that neither the expression of the *neo^r* gene itself, nor the presence of a strong promoter on the *neo^r* gene, nor the expression of -galactosidase had any dominant phenotypic consequences. The absence of any mutant phenotypes in the heterozygotes, in which the mutant allele was derived from either the father or the mother, also suggests that *int-2* is not imprinted, despite its close proximity to two other genes, H19 and Igf II, that are differentially imprinted by the two sexes (Bartolomei et al., 1991; DeChiara et al., 1991).

We found that mice homozygous for the *int-2^neo* or *int-2^lacZ* mutations often died in the early postnatal period and that they had abnormal tails and inner ears. No specific cause for the lethal effects of the mutation could be determined. One possibility is that the mutants, which were to a variable extent smaller and less well developed than their littermates, were in most cases born prematurely. This con-
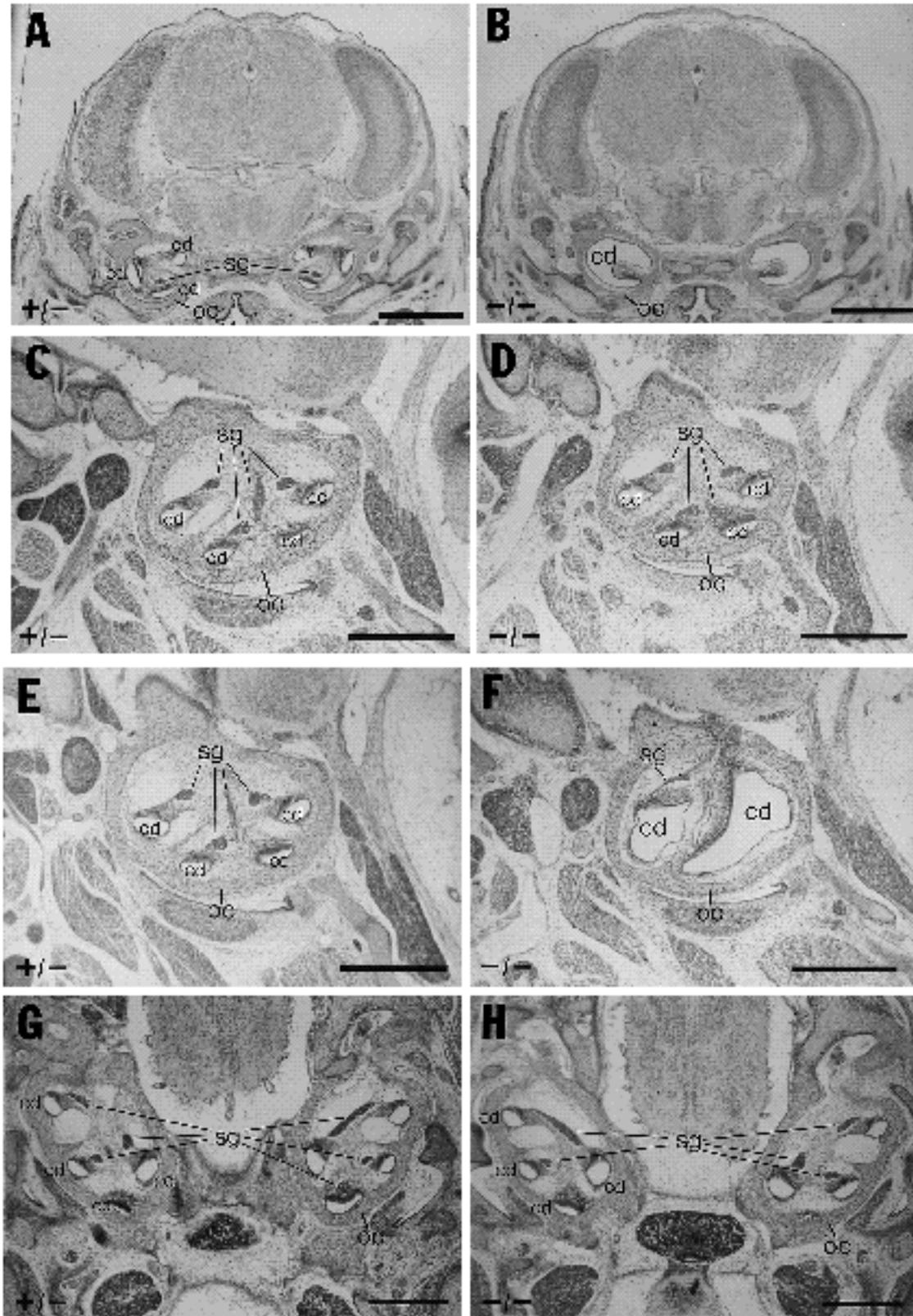
Fig. 9. Variation of the inner ear phenotype in *int-2^neo* mutant embryos. 10 µm coronal sections taken through the head of E16.5 heterozygous (A, +/−) and homozygous mutant (B, −/−) embryos. Bar, 1 mm. 10 µm sagittal sections taken through both cochleae of E16.5 heterozygous (C and E, +/−) and homozygous mutant (D and F, −/−) embryos. Bar, 0.5 mm. 10 µm transverse sections taken through the cochleae of E16.5 heterozygous (G, +/−) and homozygous mutant (H, −/−) embryos. Bar, 0.5 mm. cd (cochlear duct); sg (spiral ganglion); oc (otic capsule).
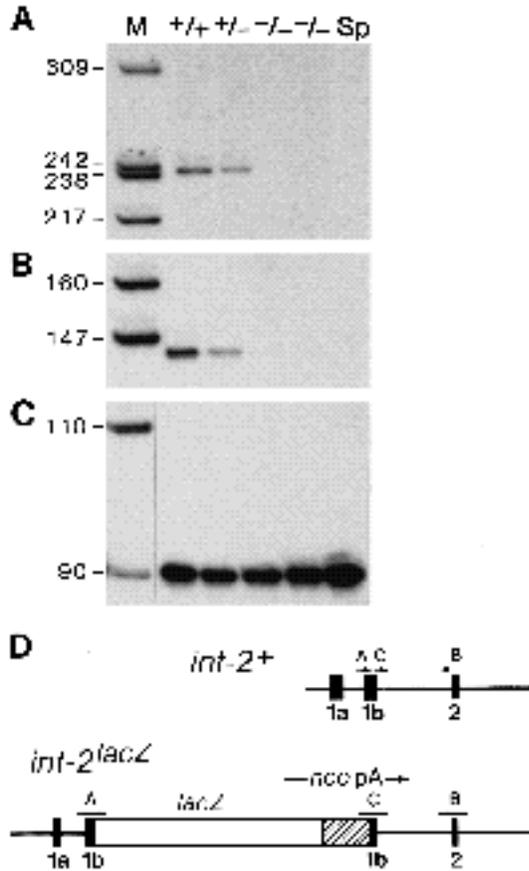
Fig. 10. RT-PCR analysis of RNA from E9.5 *int-2^{lacZ}* intercross embryos. Total RNA from E9.5 *int-2^{lacZ}* intercross embryos was reverse transcribed, cDNA was amplified in the presence of [-³²P]dCTP using three different primer pairs and the reaction products were fractionated on a sequencing gel. (A) A 241 bp reaction product with *int-2* primers A and B, which span the inserted sequences, is only detected in cDNA samples from homozygous wild-type (+/+) and heterozygous (+/−) embryos, but not in homozygous mutant (−/−) cDNA, or in adult spleen (Sp) cDNA. (B) A 145 bp reaction product with *int-2* primers C and B, which are downstream of the inserted sequences, is easily detected in cDNA samples from wild-type and heterozygous embryos, but is reduced 20- to 30-fold in cDNA samples from homozygous mutant embryos and is undetectable in adult spleen cDNA. (C) 90 bp reaction products from the actin primers are detected at approximately the same levels in all cDNA samples. (D) A map of the normal (*int-2^+*) and mutant (*int-2^{lacZ}*) *int-2* alleles showing the relative positions and orientations of the *int-2* primers A, B and C (not to scale, for the primer sequences, see Materials and methods). Darkened boxes indicate *int-2* exons, hatched boxes represent the *neo^r* gene and the open box represents the *lacZ* gene.

dition could have a direct, adverse effect their survival, or could cause the mother to segregate or kill them. Two of the surviving female homozygotes were otherwise normal and fertile. Despite the fact that *int-2* is expressed in a variety of tissues at different times during development, only two, or possibly three, of the early expression sites appear to be connected with the phenotypes of the homozygous mutant mice. Based on morphological and histological analyses, as well as on the behavior of the surviving

mutants, we found that the loss of *int-2* activity at later times in the retina, teeth and cerebellum had no obvious consequences. However, it is possible that further study of late gestation and early postnatal mutants may yet reveal a mutant phenotype that would point to the functional significance of the later *int-2* expression sites.

The *int-2^{neo}* tail phenotype

The short, curled or kinked tail phenotype, which showed 100% penetrance at E12.5 and later, is likely to be a result of the loss of *int-2* activity at an earlier stage in the primitive streak (Wilkinson et al., 1988). The posterior region of the primitive streak persists in the tail bud and is the source of tail mesenchyme (Schoenwolf, 1977). Because mutant tails are so short, one potential role for *int-2* at the 14-18 somite stage could be to stimulate the division of cells that eventually give rise to the tail bud. In addition, it is also possible that *int-2* normally functions to set up the balance between the relative rates of proliferation of different cell types that make up the tail. Thus, in the mutants, the initial dorsal direction of the curl could be explained by a more rapid rate of proliferation on the ventral side (gut endoderm) than on the dorsal side (neural tube and notochord). A third possibility is that normal *int-2* activity is required for the proper elongation of the tail by stimulation of the intercalation of mesodermal cells into a progressively narrower cell column (Weliky et al., 1991). This idea is consistent with the finding that *int-2* mutant tails are both shorter and fatter than normal tails. It is possible that the mesodermal cells which cannot form an elongated structure, exert sufficient pressure to separate the notochord from the gut tube. This abnormal cell configuration appears to affect somite formation, and hence the caudal vertebrae, which are also abnormal in the mutant tails. Further examination of the tails of normal and *int-2* mutant embryos between E9.5 and E11.5 in conjunction with studies on cell-type-specific rates of proliferation may help to choose among these possibilities.

The increased size of the neural tube in the tail may also be a consequence of the failure of the tail to elongate. The shortened tail neural tube could be subjected to increased fluid pressure, which in turn could stimulate expansion of the neuroepithelium. A similar mechanism is thought to underlie the expansion of brain tissue that occurs after the spinal canal is occluded (Desmond and Jacobson, 1977). Ultimately, since the tail neural tube is resorbed, this abnormality appears to be of little consequence to the embryo.

It is interesting to note that the tails of curly tail (*ct*) mutant mice initially curl ventrally. Upon measuring the relative rates of proliferation of different cell types in the *ct* caudal region, it was found that the gut endoderm and notochord proliferate more slowly than the neuroepithelium, surface ectoderm and mesoderm. In this case, however, the resulting ventral direction of the curling gives rise to lumbosacral neural tube defects (Copp et al., 1988; Brook et al., 1991). Although the *int-2* defect becomes apparent about a day later than the *ct* defect, it would be interesting to determine whether the double mutant combination would result in counteracting forces that might lead to a more balanced growth of the tail.

int-2 is not required for otocyst formation

Because *int-2* is expressed at E8.5-9.5 in hindbrain rhombomeres 5 and 6, which are adjacent to the developing otocyst, it seemed possible that *int-2* might be a component of the signal required to induce the otocyst to form from the otic placode. To explore this possibility, Represa et al. (1991) applied a human *int-2* anti-sense oligonucleotide (which differed by one nucleotide from the corresponding mouse sequence) to chick explants of hindbrain and otic placode. This treatment inhibited otocyst formation and the effect was correlated with the disappearance of a 31×10^3 M_r protein detected with an anti-peptide antibody raised against a highly conserved portion of the human Int-2 protein. Several considerations seem to argue against the conclusion that the effects on otocyst induction reported by Represa et al. (1991) were due to an inhibition of *int-2* function. To date, the identification of a chicken *int-2* gene has not been reported. When a mouse *int-2* probe from exon 3 was hybridized at low stringency to chicken DNA, no signal was obtained (Casey et al., 1986), whereas the probe clearly detected homologous DNA in the mammalian species tested. This result suggests that if chickens have an *int-2* gene, it may be one that has diverged significantly from mouse *int-2*. Therefore, it is unclear whether the anti-sense oligonucleotide employed by Represa et al. (1991) is in fact complementary to the chicken gene. Second, they showed no evidence that the unmodified oligonucleotide actually entered the hindbrain cells in which *int-2* is supposed to be expressed. Efficient uptake and long-term stability of oligonucleotides by untreated, intact tissues often requires that the oligonucleotide be specially modified (Akhtar and Juliano, 1992). Third, the specificity and sensitivity of the Int-2 antibody they employed is unknown. We have been unable to detect any reaction of that antibody to newborn mouse cerebellar proteins (data not shown) even though this tissue is a relatively abundant source of *int-2* mRNA (Wilkinson et al., 1989). Finally, we found that all ten of the mutant embryos that we examined at E9.5 and E10.5 had normal otocysts, suggesting that the *int-2^{neo}* mutation does not interfere with the otocyst-inducing signal.

int-2 is involved in induction of the endolymphatic duct

Our results show that the loss of *int-2* activity does have an effect on the subsequent development of the otocyst. We found that approximately 80% of the mutant embryos (60% of the mutant ears) between E11.5 and P0 had reduced or missing endolymphatic ducts. Those ears were characterized by a heterogeneous distention of the inner ear compartments (hydrops). Significantly, even in the affected regions, the epithelium had begun to differentiate sensory regions appropriately. Experimental extirpation of the endolymphatic duct has been shown to cause hydrops in chicken inner ears (Hendriks and Toerien, 1973). In those experiments, the differentiation of the sensory epithelium was not significantly affected. In addition, it is known that endolymph, produced by the stria vascularis in the cochlea, flows out of the inner ear by way of the endolymphatic duct (Guild, 1927). It is thus not surprising that removal of the structure responsible for disposal of the fluid would lead to distention of the inner ear.

The *int-2* inner ear phenotype is similar to, but less severe than, that observed in *shaker-short* (Bonnevie, 1936), *kreisler* (Deol, 1964a; Ruben, 1973), *dreher* (Deol, 1964b) and *hox 1.6* (Lufkin et al., 1991; Chisaka et al., 1992) mutant mice. The effects on the endolymphatic ducts of those mice are preceded by defects in hindbrain structure and/or alteration of the spatial relationship between the hindbrain and otocyst. We did not observe these earlier defects in *int-2* mutant mice. In addition, experimental manipulation of the hindbrain (Detwiler and Van Dyke, 1950), or grafting of the otocyst away from the hindbrain during its early development (Harrison, 1936; Detwiler and Van Dyke, 1950; Detwiler and Van Dyke, 1951) have also been correlated with defects in endolymphatic duct formation. These results suggest that in addition to the hindbrain signal required to induce the otocyst to form, there are additional interactions necessary for induction of the endolymphatic duct. From the phenotype of *int-2* mutant mice, we suggest that *int-2* is a component of the latter inductive signal rather than the former. The more severe phenotypes of the mutants mentioned above could be interpreted as resulting from interference with the normal hindbrain/otocyst apposition required for the transmission of inducing signals, rather than interference with the signaling molecules themselves.

Although it is attractive to suppose that *int-2* expression in the hindbrain is involved in inducing the endolymphatic duct, it remains a possibility that the relevant *int-2* expression site is not the hindbrain, but rather the otocyst itself. Recall that *int-2* is expressed in the prospective vestibular sensory cells at E10.5 (Wilkinson et al., 1989). We cannot exclude the possibility that this *int-2* expression site is responsible for induction of the endolymphatic duct and the subsequent morphogenesis of the inner ear. We are currently trying to determine whether expression of *int-2* in the hindbrain and otocyst is differentially regulated, with the aim of producing and analyzing mice that lack *int-2* expression in only one or the other location. Meanwhile, further examination of the *int-2^{neo}/int-2^{lacZ}* mice may help to clarify this issue.

We found that the distended inner ears seen in older embryos were often deficient in spiral ganglion cells. While this may have been partly a physical consequence of the expansion of the inner ear leaving no space for the spiral ganglion cells, we did note that some E10.5 and E11.5 mutant ears showed an apparent reduction in the size of the VIIIth ganglion, prior to the ballooning of the cochlea. This observation needs further documentation, but it is consistent with the possibility that *int-2* expression in the otocyst at E10.5 is involved in stimulating the production or migration of VIIIth ganglion cells (Wilkinson et al., 1989), which are derived from the otic epithelium (Altman and Bayer, 1982; Noden and Van De Water, 1986). Expression of *int-2* in the sensory regions of the developing ear seems, however, to be unrelated to their differentiation because even the most abnormally shaped *int-2* mutant inner ears showed appropriate sensory differentiation. Whether the innervation of the sensory hair cells is affected needs further examination, but on a gross level the observed ganglion cells present did appear to send processes to the appropriate sensory epithelium.

Variable expression of the *int-2* inner ear mutant phenotype

In contrast to the tail phenotype, we found that the *int-2* inner ear phenotype showed variation in both penetrance and expressivity. In the case of recessive mutations, such properties are usually attributed to the segregation of modifying genes in a non-uniform genetic background and/or to leaky expression of the mutant gene. Neither of these explanations seems attractive in this case. The instances of extreme variation between development of right and left ears of individual mutant mice argue strongly against any explanation based only on genetic background. Leaky expression also seems unlikely here, since the *int-2^neo^* allele used is expected to be a null mutation for several reasons. First, the position of the inserted sequences in exon 1b prevents production of a full length Int-2 protein. Second, mice homozygous for an independently derived *int-2* allele, *int-2^lacZ^*, display identical phenotypes to those reported for the *int-2^neo^* mutation. The *lacZ/neo^r^* insertion in these mice is also located in exon 1b, fusing *int-2* and *lacZ* sequences, and should also interfere with production of full-length Int-2 protein. Indeed, we found that *int-2^lacZ^* homozygous mutant embryos did not produce transcripts linking the translation initiation codon and signal peptide upstream of the inserted DNA with downstream exons.

One possible explanation for the variability in the ear phenotype is that there could be parallel signaling pathways for inner ear development and that utilization of these pathways in a single individual is mosaic, resulting in variable success in complementing the loss of *int-2* function. Interestingly, we are finding that variability in the expressivity of mutant phenotypes that result from presumed null mutations in other mouse developmental genes, appears to be the norm rather than the exception [see for example, *wnt-1* (Thomas and Capecchi, 1990), *sw* (Thomas et al., 1991), *hox 1.5* (Chisaka and Capecchi, 1991) and *hox 1.6* (Chisaka et al., 1992)]. In the present case, the proposed parallel signaling pathways could involve signals related to *int-2*, such as other members of the FGF family. The absence of *int-2* would then often result in defects of inner ear development, but occasionally, on a stochastic basis, the *int-2* pathway could be activated by another signal. Presumably, such parallel pathways do not operate in the primitive streak mesoderm in which *int-2* expression is required for normal tail formation, because this tissue is always affected by the *int-2* mutation. The absence of any mutant phenotypes attributable to the loss of *int-2* at later times might then be due to complete functional redundancy in the *int-2* signaling pathway at later developmental stages. The phenotypes of mice mutant for other members of the FGF family and their receptors, as well as the various double mutant combinations should shed light on this issue.

REFERENCES

Acland, P., Dixon, M., Peters, G. and Dickson, C. (1990). Subcellular fate of the Int-2 oncoprotein is determined by choice of initiation codon. *Nature* **343**, 662-665.

Akhtar, S. and Juliano, R. L. (1992). Cellular uptake and intracellular fate of antisense oligonucleotides. *Trends Cell Biol.* **2**, 139-144.

Altman, J. and Bayer, S. (1982). Development of the cranial nerve ganglia and related nuclei in the rat. *Adv. Anat. Embryol. Cell Biol.* **74**, 1-90.

Baird, A. and Klagsbrun, M. (1991). The fibroblast growth factor family: an overview. *Ann. N. Y. Acad. Sci.* **638**, xi-xvi.

Bartolomei, M. S., Zemel, S. and Tilghman, S. M. (1991). Parental imprinting of the mouse H19 gene. *Nature* **351**, 153-155.

Bonnevie, K. (1936). Abortive differentiation of the ear vesicles following a hereditary brain-anomaly in the 'short-tailed walzing mice'. *Genetica* **18**, 105-125.

Brook, F. A., Shum, A. S., Van Straaten, H. W. M. and Copp, A. J. (1991). Curvature of the caudal region is responsible for failure of neural tube closure in the curly tail (*ct*) mouse embryo. *Development* **113**, 671-678.

Burgess, W. H. and Maciag, T. (1989). The heparin-binding fibroblast growth factor family of proteins. *Ann. Rev. Biochem.* **58**, 575-606.

Casey, G., Smith, R., McGillivray, D., Peters, G. and Dickson, C. (1986). Characterization and chromosome assignment of the human homolog of *int-2*, a potential proto-oncogene. *Mol. Cell. Biol.* **6**, 502-510.

Cathala, G., Savouret, J.-F., Mendez, B., West, B. L., Karin, M., Martial, J. A. and Baxter, J. D. (1983). A method for isolation of intact, translationally active ribonucleic acid. *DNA* **2**, 329-335.

Chisaka, O. and Capecchi, M. R. (1991). Regionally restricted developmental defects resulting from targeted disruption of the mouse homeobox gene *hox-1.5*. *Nature* **350**, 473-479.

Chisaka, O., Musci, T. S. and Capecchi, M. R. (1992). Developmental defects of the ear, cranial nerves and hindbrain resulting from targeted disruption of the mouse homeobox gene *Hox-1.6*. *Nature* **355**, 516-520.

Church, G. M. and Gilbert, W. (1984). Genomic sequencing. *Proc. Nat. Acad. Sci. USA* **81**, 1991-1995.

Copp, A. J., Brook, F. A., Estibeiro, J. P., Shum, A. S. W. and Cockroft, D. L. (1990). The embryonic development of mammalian neural tube defects. *Prog. Neurobiol.* **35**, 363-403.

Copp, A. J., Brook, F. A. and Roberts, H. J. (1988). A cell-type-specific abnormality of cell proliferation in mutant (curly tail) mouse embryos developing spinal neural tube defects. *Development* **104**, 285-295.

DeChiara, T. M., Robertson, E. J. and Efstratiadis, A. (1991). Parental imprinting of the mouse insulin-like growth factor II gene. *Cell* **64**, 849-859.

Deol, M. S. (1964a). The abnormalities of the inner ear in *kreisler* mice. *J. Embryol. Exp. Morph.* **12**, 475-490.

Deol, M. S. (1964b). The origin of the abnormalities of the inner ear in *dreher* mice. *J. Embryol. Exp. Morph.* **12**, 727-733.

Deol, M. S. (1968). Inherited diseases of the inner ear in man in the light of studies on the mouse. *J. Med. Genet.* **5**, 137-154.

Deol, M. S. (1980). Genetic malformations of the inner ear in the mouse and in man. In *Morphgenesis and Malformation of the Ear* (ed. R. J. Gorlin) pp. 243-259. New York: Alan R. Liss, Inc.

Desmond, M. E. and Jacobson, A. G. (1977). Embryonic brain enlargement requires cerebrospinal fluid pressure. *Dev. Biol.* **57**, 188-198.

Detwiler, S. R. and Van Dyke, R. H. (1950). The role of the medulla in the differentiation of the otic vesicle. *J. Exp. Zool.* **113**, 179-199.

Detwiler, S. R. and Van Dyke, R. H. (1951). Recent experiments on the differentiation of the labyrinth in Amblystoma. *J. Exp. Zool.* **118**, 389-401.

Dickson, C. and Peters, G. (1987). Potential oncogene product related to growth factors. *Nature* **326**, 833.

Dickson, C., Smith, R., Brookes, S. and Peters, G. (1984). Tumorigenesis by Mouse Mammary Tumor Virus: proviral activation of a cellular gene in the common integration region *int-2*. *Cell* **37**, 529-536.

Dingerkus, G. and Uhler, L. D. (1977). Enzyme clearing of alcian blue-stained whole small vertebrates for demonstration of cartilage. *Stain Technol.* **52**, 229-232.

Dodd, J., Morton, S. B., Karagogeos, D., Yamamoto, M. and Jessell, T. M. (1988). Spatial regulation of axonal glycoprotein expression on subsets of embryonic spinal neurons. *Neuron* **1**, 105-116.

Goldfarb, M. (1990). The fibroblast growth factor family. *Cell Growth and Diff.* **1**, 439-445.

Guild, S. R. (1927). The circulation of the endolymph. *Amer. J. Anat.* **39**, 57-81.

Harrison, R. G. (1936). Relations of symmetry in the developing ear of Amblystoma punctatum. *Proc. Natl. Acad. Sci. USA* **22**, 238-247.

Hendriks, D. M. and Toerien, M. J. (1973). Experimental endolymphatic hydrops. *S. Afr. Med. J.* **47**, 2294-2298.

Hogan, B., Constantini, F. and Lacy, E. (1986). *Manipulating the Mouse Embryo.* Cold Spring Harbor: Cold Spring Harbor Laboratory.

Jakobovits, A., Shackleford, G. M., Varmus, H. E. and Martin, G. R. (1986). Two proto-oncogenes implicated in mammary carcinogenesis, *int-1* and *int-2* are independently regulated during mouse development. *Proc. Natl. Acad. Sci. USA* **83**, 7806-7810.

Kaufman, M. H. (1990). Morphological stages of postimplantation embryonic development. In *Postimplantation Mammalian Embryos: a Practical Approach* (ed. A. J. Copp and D. L. Cockroft) pp. 81-91. New York: Oxford University Press.

Lufkin, T., Dierich, A., LeMeur, M., Mark, M, and Chambon, P. (1991). Disruption of the *Hox-1.6* homeobox gene results in defects in a region corresponding to its rostral domain of expression. *Cell* **66**, 1105-1119.

Mansour, S. L. and Martin, G. R. (1988). Four classes of mRNA are expressed from the mouse *int-2* gene, a member of the FGF gene family. *EMBO J.* **7**, 2035-2041.

Mansour, S. L., Thomas, K. R. and Capecchi, M. R. (1988). Disruption of the proto-oncogene *int-2* in mouse embryo-derived stem cells: a general strategy for targeting mutations to non-selectable genes. *Nature* **336**, 348-352.

Mansour, S. L., Thomas, K. R., Deng, C. X. and Capecchi, M. R. (1990). Introduction of a *lacZ* reporter gene into the mouse *int-2* locus by homologous recombination. *Proc. Natl. Acad. Sci. USA* **87**, 7688-7692.

McLeod, M. J. (1980). Differential staining of cartilage and bone in whole mouse fetuses by alcian blue and alizarin red S. *Teratol.* **22**, 299-301.

Muller, W. J., Lee, F. S., Dickson, C., Peters, G., Pattengale, P. and Leder, P. (1990). The *int-2* gene product acts as an epithelial growth factor in transgenic mice. *EMBO J.* **9**, 907-913.

Niswander, L. and Martin, G. R. (1992). *Fgf-4* expression during gastrulation, myogenesis, limb and tooth development in the mouse. *Development* **114**, 755-768.

Noden, D. M. and Van De Water, T. R. (1986). The developing ear: tissue origins and interactions. In *The Biology of Change in Otolaryngology* (ed. R. J. Ruben, T. R. Van De Water and E. W. Rubel) pp. 15-46. Amsterdam: Elsevier.

Represa, J., Leon, Y., Miner, C. and Giraldez, F. (1991). The *int-2* proto-oncogene is responsible for induction of the inner ear. *Nature* **353**, 561-563.

Ruben, R. J. (1973). Development and cell kinetics of the kreisler (kr/kr) mouse. *Laryngoscope* **83**, 1440-1468.

Rugh, R. (1968). *The Mouse: its Reproduction and Development.* Minneapolis: Burgess.

Ruoslahti, E. and Yamaguchi, Y. (1991). Proteoglycans as modulators of growth factor activities. *Cell* **64**, 867-869.

Sanes, J. R., Rubenstein, J. L. R. and Nicolas, J.-F. (1986). Use of a recombinant retrovirus to study post-implantation cell lineage in mouse embryos. *EMBO J.* **5**, 3133-3142.

Schoenwolf, G. (1984). Histological and ultrastructural studies of secondary neurulation in mouse embryos. *Am. J. Anat.* **169**, 361-376.

Schoenwolf, G. C. (1977). Tail (end) bud contributions to the posterior region of the chick embryo. *J. Exp. Zool.* **201**, 227-246.

Sher, A. E. (1971). The embryonic and postnatal development of the inner ear of the mouse. *Acta Otolaryngol.* **285 Supplement**, 1-77.

Steel, K., Niaussal, M.-M. and Bock, G. R. (1983). The genetics of hearing. In *The Auditory Psychobiology of the Mouse* (ed. J. F. Willott) pp. 341-394. Springfield: C. C. Thomas.

Tan, S. S. and Weis, J. H. (1992). Development of a sensitive reverse transcriptase PCR assay, RT-PCR, utilizing rapid cycle times. *PCR Meth. Appl.* (in press).

Theiler, K. (1989). *The House Mouse. Development and Normal Stages from Fertilization to 4 Weeks of Age.* Berlin: Springer-Verlag.

Thomas, K. R. and Capecchi, M. R. (1987). Site-directed mutagenesis by gene targeting in mouse embryo-derived stem cells. *Cell* **51**, 503-512.

Thomas, K. R. and Capecchi, M. R. (1990). Targeted disruption of the murine int-1 proto-oncogene resulting in severe abnormalities in midbrain and cerebellar development. *Nature* **346**, 847-850.

Thomas, K. R., Musci, T. A., Neumann, P. E. and Capecchi, M. R. (1991). Swaying is a mutant allele of the proto-oncogene *Wnt-1. Cell* **67**, 969-976.

Van De Water, T. R., Li, C. W., Ruben, R. J. and Shea, C. A. (1980). Ontogenic aspects of mammalian inner ear development. In *Morphogenesis and Malformation of the Ear* (ed. R. J. Gorlin) pp. 5-45. New York: Alan R. Liss, Inc.

Van De Water, T. R. and Represa, J. (1991). Tissue interactions and growth factors that control development of the inner ear. *Ann. N. Y. Acad. Sci.* **630**, 116-128.

Van De Water, T. R. and Ruben, R. J. (1976). Organogenesis of the ear. In *Scientific Foundations of Otolaryngology* (ed. R. Hinchcliffe and D. Harrison) pp. 173-184. London: William Heineman Medical Books Ltd.

Weliky, M., Minsuk, S., Keller, R. and Oster, G. (1991). Notochord morphogenesis in *Xenopus laevis*: simulation of cell behavior underlying tissue convergence and extension. *Development* **113**, 1231-1244.

Wilkinson, D. G., Bhatt, S. and McMahon, A. P. (1989). Expression pattern of the FGF-related proto-oncogene *int-2* suggests multiple roles in fetal development. *Development* **105**, 131-136.

Wilkinson, D. G., Peters, G., Dickson, C. and McMahon, A. P. (1988). Expression of the FGF-related proto-oncogene *int-2* during gastrulation and neurulation in the mouse. *EMBO J.* **7**, 691-695.